Molecular Neurobiology (2019) 56:5749–5762
https://doi.org/10.1007/s12035-019-1473-x

Ethanol Exposure Transiently Elevates but Persistently Inhibits Tyrosine Kinase Activity and Impairs the Growth of the Nascent Apical Dendrite

Dandan Wang[1,2] · Joshua Enck[1,2] · Brian W. Howell[1] · Eric C. Olson[1,2]

Received: 4 September 2018 / Accepted: 10 January 2019 / Published online: 23 January 2019

Abstract

Dendritogenesis can be impaired by exposure to alcohol, and aspects of this impairment share phenotypic similarities to dendritic defects observed after blockade of the Reelin-Dab1 tyrosine kinase signaling pathway. In this study, we find that 10 min of alcohol exposure (400 mg/dL ethanol) by itself causes an unexpected increase in tyrosine phosphorylation of many proteins including Src and Dab1 that are essential downstream effectors of Reelin signaling. This increase in phosphotyrosine is dose-dependent and blockable by selective inhibitors of Src Family Kinases (SFKs). However, the response is transient, and phosphotyrosine levels return to baseline after 30 min of continuous ethanol exposure, both in vitro and in vivo. During this latter period, Src is inactivated and Reelin application cannot stimulate Dab1 phosphorylation. This suggests that ethanol initially activates but then silences the Reelin-Dab1 signaling pathway by brief activation and then sustained inactivation of SFKs. Time-lapse analyses of dendritic growth dynamics show an overall decrease in growth and branching compared to controls after ethanol-exposure that is similar to that observed with Reelin-deficiency. However, unlike Reelin-signaling disruptions, the dendritic filopodial speeds are decreased after ethanol exposure, and this decrease is associated with sustained dephosphorylation and activation of cofilin, an F-actin severing protein. These findings suggest that persistent Src inactivation coupled to cofilin activation may contribute to the dendritic disruptions observed with fetal alcohol exposure.

Keywords Fetal alcohol syndrome disorder · Cortical development · Src kinases · Dab1 · Dendritogenesis · Cofilin

Introduction

Fetal alcohol spectrum disorder (FASD) is estimated to affect between 1 and 5% of all births in the USA and is a leading cause of intellectual disability in children [1]. Children prenatally exposed to alcohol present with a number of functional deficits reflective of abnormal cortical development [2, 3] including significant disruptions of the neurites and synapses that make up the functional circuitry of the brain. While there are many alcohol sensitive developmental events (e.g., neuronal proliferation and migration) that would be expected to alter the later development of neuronal wiring and later brain function [4, 5], there is also evidence for direct effects of alcohol on the development and plasticity of axons and dendrites [6–8].

To better understand the consequence of alcohol exposure on dendritogenesis, we have focused on a particularly dynamic period of development, the period of apical dendritic initiation. Studies in rodents have shown that the cortical apical dendrite is initiated by direct transformation of the leading process of the migrating neuron, during the last 2 h of the migration period [9]. During this period, the total neurite arbor size and branching increase 2.5- to 3-fold, the neuron arrests migration and begins to develop electrical properties characteristic of maturing neurons [10]. Unsurprisingly, dendritogenesis is associated with the expression of hundreds of genes associated with neuronal differentiation [11]. This biological dynamism renders the neuron particularly susceptible to ethanol (EtOH) exposure during this period as prior studies have shown that dendritic outgrowth is sensitive to EtOH exposure depending on cell class and exposure paradigm [12–15].

In a prior study, we found that the growing apical dendrite of cortical neurons showed altered branching and growth after as little as 4 h of ethanol exposure. This altered dendritic

Electronic supplementary material The online version of this article (https://doi.org/10.1007/s12035-019-1473-x) contains supplementary material, which is available to authorized users.

✉ Eric C. Olson
olsone@upstate.edu

[1] Department of Neuroscience and Physiology, SUNY Upstate Medical University, 505 Irving Ave, Syracuse, NY 13210, USA

[2] Developmental Exposure to Alcohol Research Center (DEARC), Binghamton University, Binghamton, NY 13902, USA

structure was accompanied by a compacted Golgi apparatus and altered expression of MAP 2, a microtubule-associated protein that is highly expressed in the dendrite [16]. This constellation of defects was similar to, albeit less severe, than disruptions observed in Reelin-deficient cortices of reeler mice [17]. Reelin is a secreted glycoprotein that binds two receptors (VLDLR and ApoER2) expressed on developing cortical neurons. This binding causes receptor clustering and the activation of Src Family Kinases (SFKs) members Src and Fyn, leading to tyrosine phosphorylation of Dab1, a critical cytoplasmic adaptor protein, that coordinates biochemical signaling supporting migration termination and dendritic initiation and growth [18, 19]. Importantly, mouse embryos deficient in two SFKs (Src and Fyn) show reeler-like cortical disruptions [20], a finding that identifies the essential requirement for these SFKs in Reelin-signaling and emphasizes the point that embryonic disruptions of the activity of these kinases would disrupt Reelin-signaling.

To determine the potential impact of EtOH exposure on Reelin-Dab1 signaling, we examined the acute cellular and biochemical response of differentiating cortical neurons to single-dose EtOH exposure. Using organotypic explants and primary neuronal cultures, live-cell imaging revealed a rapid alteration of dendritic growth after EtOH exposure. This dendritic disruption temporally coincides with a transient increase in tyrosine phosphorylation of multiple proteins, including Src and Dab1, proteins involved in Reelin-signaling dependent dendritic initiation and stabilization. These initial phosphorylation events are almost completely blocked by SFK inhibitors indicating that EtOH exposure can rapidly activate this important family of kinases. However, the phosphotyrosine levels return to baseline after 30 min of continuous ethanol exposure, and SFK activation loop phosphorylation drops below baseline, suggesting SFKs are inactivated in the later period of the EtOH response. After this rapid initial activation, Reelin application cannot stimulate Dab1 phosphorylation suggesting that ethanol silences the Reelin-Dab1 signaling pathway by inactivating SFKs. In addition, a sustained dephosphorylation and activation of the F-actin severing protein cofilin is observed in the presence of EtOH, which likely contributes to the observed disruption of the nascent dendrite.

Results

Ethanol exposure causes a rapid increase in phosphotyrosinated proteins

Tyrosine kinase signaling pathways have critical roles in dendritic growth and branching [21–24]. To determine whether EtOH exposure alters basal phosphotyrosine content, E15 wildtype cortical neuron cultures were prepared and exposed to 0.5% *v*/*v* EtOH for different time periods on DIV3 (in vitro day 3). Western blot analyses revealed a surprising ~ 5-fold total increase in phosphotyrosine immunoreactivity (pY99 antibody) across multiple molecular weight proteins at 10 min after EtOH exposure compared to control (Fig. 1a**)**. Interestingly, the phosphotyrosine response was transient and largely absent after 30 + min of continuous EtOH exposure (Fig. 1c). Calcein AM and propidium iodide assay (live/dead assay) of parallel cortical cultures confirmed that continuous exposure of this concentration of EtOH (equivalent to 400 mg/dL) did not negatively impact cell health over a 16-h period compared to controls (Supplemental Fig. 1a, b). The dose-response relationship between EtOH and phosphotyrosine immunoreactivity was tested at the 10-min exposure time point and showed a steady increase starting at 0.125% EtOH and continuing up to the maximum tested concentration, 0.75% EtOH (Fig. 1b, d, $^{*}p < 0.05$; $^{\#}p < 0.001$).

Reelin signaling stabilizes the developing cortical dendrite [17, 19, 25–27] through activation of SFK members Src and Fyn and the tyrosine phosphorylation of the cytoplasmic adapter protein Dab1 [28, 29]. To determine whether the increased phosphotyrosine included Reelin signaling components, Src, Fyn, and Dab1 were immunoprecipitated from these lysates and then probed using the anti-pY416 Src/Fyn activation loop antibody and separately the anti-pY99 antibody to identify phosphorylated Dab1 in the Dab1 immunoprecipitate (Fig. 1e–g). Increased phosphotyrosine levels of Src and Dab1 were observed after EtOH exposure suggesting that EtOH may initially activate the SFK-Dab1 signaling. (pSrc 1.0 ± 0.1 in H_2O vs. 1.4 ± 0.01 in EtOH, $^{*}p < 0.05$; pDab1 0.9 ± 0.1 in H_2O vs. 9.7 ± 0.5 in EtOH, $^{\#}p < 0.0001$; Fig. 1h, j). In contrast, we did not detect a significant alteration in Fyn activation loop phosphorylation after total Fyn immunoprecipitation (Fig. 1f, i).

The Ethanol-Response Is Blocked by Kinase Inhibitors but Is Not Affected by a Phosphatase Inhibitor

An increase in pY416 Src activation loop phosphorylation raised the possibility that the increased tyrosine phosphorylation was due to activation of SFKs. To determine the total increase in phosphotyrosine (pY99 western signal) attributable to SFKs activation, dissociated E15 cortical cultures were pretreated for 30 min with 20 μM PP2, a specific inhibitor of SFKs, or the same concentration of the inactive enantiomer PP3 [30] and then exposed to 0.5% EtOH. As shown in Fig. 2a, addition of PP2 blocks the majority of ethanol-induced tyrosine phosphorylation (1.5 ± 0.1 in PP2 + EtOH vs. 4.9 ± 0.4 in EtOH, $^{\#}p = 0.0004$; Fig. 2b) while PP3 had no effect on the EtOH response (data not shown). A second SFK inhibitor, SKI-1 also blocked the ethanol-induced response (Fig. 2c, d). As SFK inhibitors like PP2 can also block the non-receptor tyrosine kinase Abl, imatinib, (STI-571), which inhibits Abl but not SFKs was also tested. Imatinib did not block the

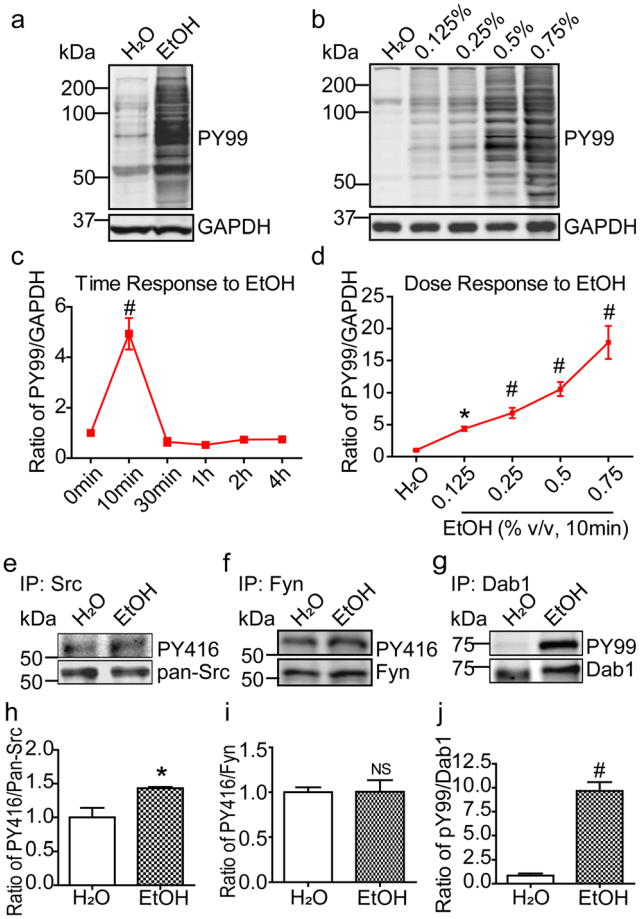

Fig. 1 Rapid and transient tyrosine phosphorylation of multiple proteins in response to ethanol. **a** 10 min of 0.5% EtOH exposure induced an increase in tyrosine phosphorylation of multiple proteins from cultured embryonic cortical cells. **b** Dose-dependent increase of tyrosine phosphorylation in response to 10 min of EtOH. **c** Time course of 0.5% EtOH-induced tyrosine phosphorylation. Tyrosine phosphorylation level was determined by western blot using an anti-phosphotyrosine antibody (pY99). Densitometric values were expressed as total pY99/GAPDH, and then normalized to H_2O group for each concentration. **d** Dose response of EtOH-induced tyrosine phosphorylation at 10 min normalized to H_2O control. **e**–**g** EtOH exposure increased Src activation loop and Disabled 1 (Dab1) tyrosine-phosphorylation levels. After 10 min of 0.5% EtOH exposure, total Src, Fyn, or Dab1 protein were immunoprecipitated from E15 cortical lysates and **e**, **f** Src/Fyn activation (pY416), or **g** Dab1 phosphorylation (pY99) was determined. **h**–**j** Quantification of blots revealed a significant increase of **h** Src activation and **j** Dab1 phosphorylation after EtOH exposure, indicating activation of these elements of the Reelin-signaling pathway. One-way ANOVA with Bonferroni post-hoc test was performed between different time points or concentration in **c** and **d**. *t* test was used to compare the differences between H_2O and EtOH group in **g** and **h**. $^{*}p < 0.05$, $^{\#}p < 0.001$, NS, $p > 0.05$

increased tyrosine phosphorylation induced by EtOH (3.7 ± 0.61 in imatinib + EtOH vs. 4.7 ± 0.71 in EtOH, $p > 0.05$; Fig. 2d). To examine the possibility that EtOH also decreases tyrosine phosphatase activity, 20 μM phenylarsine oxide (PAO), a membrane-permeable inhibitor of class I phosphotyrosine phosphatases [31], was added to the cortical culture 30, 40, or 60 min before 0.5% EtOH exposure. In H_2O group, PAO caused a detectable increase in basal tyrosine phosphorylation without any additional stimulation indicating the efficacy of PAO (1.0 ± 0.1 in H_2O vs. 3.4 ± 0.3 in PAO; $^{**}p < 0.01$; Fig. 2e, f). However, pretreatment with PAO for 30 or 40 min did not inhibit EtOH's effect (30 min, 2.5 ± 0.4 in PAO vs. 5.1 ± 0.1 in PAO + EtOH; $^{\#}p < 0.001$; 40min, 2.7 ± 0.4 in PAO vs. 4.8 ± 0.3 in PAO + EtOH; $^{**}p < 0.01$; Fig. 2f). Taken together, these results suggest that activation of PP2-sensitive tyrosine kinases, rather than inhibition of tyrosine phosphatases, is largely responsible for the increased tyrosine phosphorylation observed 10 min after EtOH exposure.

EtOH, as a hydrophilic solvent, has been reported to intercalate into lipid bilayers, increasing membrane fluidity and change membrane polarization [32–34]. Membrane fluidity may be related to the activation of kinases as cholesterol enriched lipid rafts are often signaling centers on the cell surface, and clustering of SFKs by Dab1 binding is sufficient to activate the SFKs [35, 36]. However, neither addition of cholesterol nor cholesterol depletion using methyl-β-cyclodextrin significantly altered the response of cultured neurons to EtOH (Supplemental Fig. 1c and d). This suggests that altered membrane fluidity and/or changes in lipid raft composition may not have a major role in EtOH-dependent activation of SFKs.

Ethanol Exposure Decreases Neurite Extension and Retraction Velocities in Culture

To better correlate dendritic dynamics with our biochemical findings, we examined dendritic dynamics in culture. Prior studies indicated that 0.25, 0.5, and 0.75%-sustained EtOH exposure inhibited both dendritic growth and later synapse formation in hippocampal neuron cultures [6]. To label immature cortical neurons, we prepared whole hemisphere explants after ex utero electroporation of a dsRed expression construct (Dcx-dsRed). Electroporation on E13 labels early born deep layer neurons that differentiate during a 2-day culture period in vitro. The explants were then dissociated and cultured for subsequent time-lapse confocal imaging. The total dendritic arbor was traced from the data sets at 30-min intervals before and after EtOH or H_2O application. The control H_2O group demonstrated a balance between neurite elongations and retractions but showed a slight decrease in overall dendritic arbor size and branching throughout the imaging period (Fig. 3a–c). In contrast, EtOH exposure caused a dramatic decrease in dendritic arbor size, with a 53% reduction of total dendrite length ($EtOH_{-60\ min} = 386.9 \pm 29.2$, $EtOH_{180\ min} = 180.6 \pm 30.4$ vs. $H_2O_{180\ min} = 307.9 \pm 28.1$, $^{**}p < 0.01$, Fig. 3b, a) and a ~41% decrease of branch number ($EtOH_{-60\ min} = 11.9 \pm 0.8$ vs. $EtOH_{180\ min} = 7 \pm 0.9$, Fig. 3c) after 3 h of exposure, values that are significantly different from control ($EtOH_{180\ min} = 7 \pm 0.9$ vs. $H_2O_{180\ min} = 12.1 \pm 1.2$, $^{**}p < 0.001$, Fig. 3c). The total number of neurite movements (events) showed a significant decrease at 30 min and

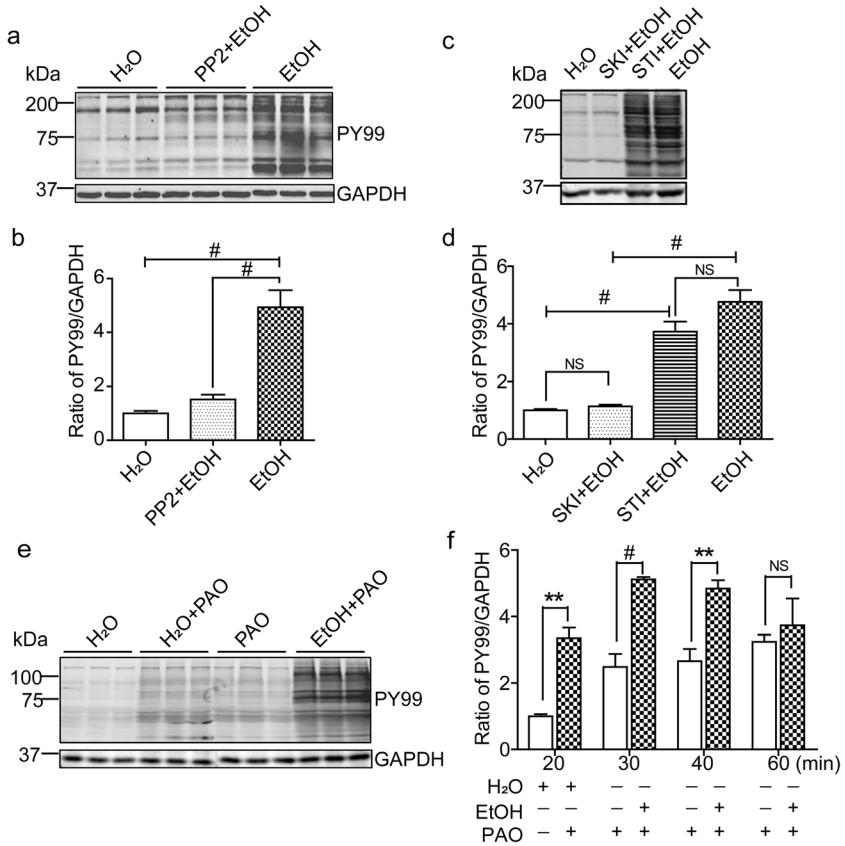

Fig. 2 Ethanol-induced upregulation of tyrosine phosphorylation is dependent on Src family kinase but not phosphatase activity. **a**, **b** EtOH-induced tyrosine phosphorylation was blocked by pretreatment with the Src kinase inhibitor PP2. E15 cortical cultures were treated with 20 μM PP2 or same concentration of the inactive enantiomer PP3 (data not shown) for 30 min before EtOH exposure (0.5%, 10 min). **c**, **d** Ethanol-induced increase in tyrosine phosphorylation could be blocked by the SFKs inhibitor 1 (SKI-1), but not Abl kinase inhibitor STI-571. E15 cortical cultures were pretreated with SKI-1(100 nM, 30 min) or STI-571 (1 μM, 1 h) before 10 min of 0.5% EtOH exposure. Cells were lysed and subjected to western blot analysis with the indicated antibodies. **e**–**f** Tyrosine phosphorylation after EtOH exposure was not blocked by phosphatase inhibitor pretreatment. Cultures were pretreated with 20 μM phenylarsine oxide (PAO) for varying times (30 min, 40 min, 60 min) prior to 10 min of 0.5% EtOH exposure. One-way ANOVA with Bonferroni post-hoc test was performed between different groups. $^{**}p < 0.01$, $^{\#}p < 0.001$, NS, $p > 0.05$

was reduced ~53% by the end of the 3-h exposure period ($EtOH_{180\ min} = 9 \pm 1$ vs. $EtOH_{-30\ min} = 19 \pm 1.5$, $^{\#}p < 0.001$ when compared with $H_2O_{180\ min}$, Fig. 3d). The EtOH-exposed dendritic filopodia were more stable with more stall events ($EtOH_{150\ min} = 24.8\% \pm 4.2\%$ vs. $H_2O_{150\ min} = 3.3\% \pm 2.3\%$, $^{\#}p < 0.001$; $EtOH_{180\ min} = 15.7\% \pm 6.7\%$ vs. $H_2O_{180\ min} = 2.5\% \pm 1.1\%$, $^{*}p < 0.05$, Fig. 3e) and slower extension and retraction speeds as compared to control ($H_2O_{60\ min} = 38 \pm 4$ μm/h vs. $EtOH_{60\ min} = 14 \pm 2.8$, $^{\#}p = 0.0005$, Fig. 3f). The reduced extension and retraction dynamics persisted throughout the imaging period ($^{**}p < 0.01$, $^{\#}p < 0.001$, Fig. 3f). Thus, quantitatively, EtOH-exposure greatly reduced dendritic filopodial dynamics, and the major driver of overall arbor size reduction was a proportionately greater decrease in filopodial extension speed and fewer extension events compared to control.

As PP2 blocks EtOH-induced tyrosine phosphorylation, we next asked whether PP2 could protect against EtOH-induced neurite collapse. Twenty micromolar PP2 was applied to cortical primary cultures for 30 min before EtOH dosing. Quantification of total neurite size and branching revealed a significant block of EtOH-effects on growth rate, but not branching 1h after EtOH exposure ($PP2 + EtOH_{60\ min} = 76.2 \pm 3.3$ vs. $EtOH_{60\ min} = 56.3 \pm 4.2$, $^{*}p < 0.05$, Fig. 3g). However, this modest neuroprotection was lost at later time points after exposure (Fig. 3g, h), suggesting that PP2 blunts only the initial growth inhibition of EtOH.

Aberrant Cofilin Activation May Mediate Ethanol-Induced Actin Dynamics Disruption Through Src Inactivation

Cofilin is an effector of Reelin-signaling downstream of SFKs [37] and a key regulator of actin dynamics in the maturing neuron as reductions in the level of cofilin activity profoundly restrict neurite outgrowth [38]. Although cofilin severs actin filaments, the free barbed ends can then act as new binding sites for the active Arp2/3 complex and new actin branches

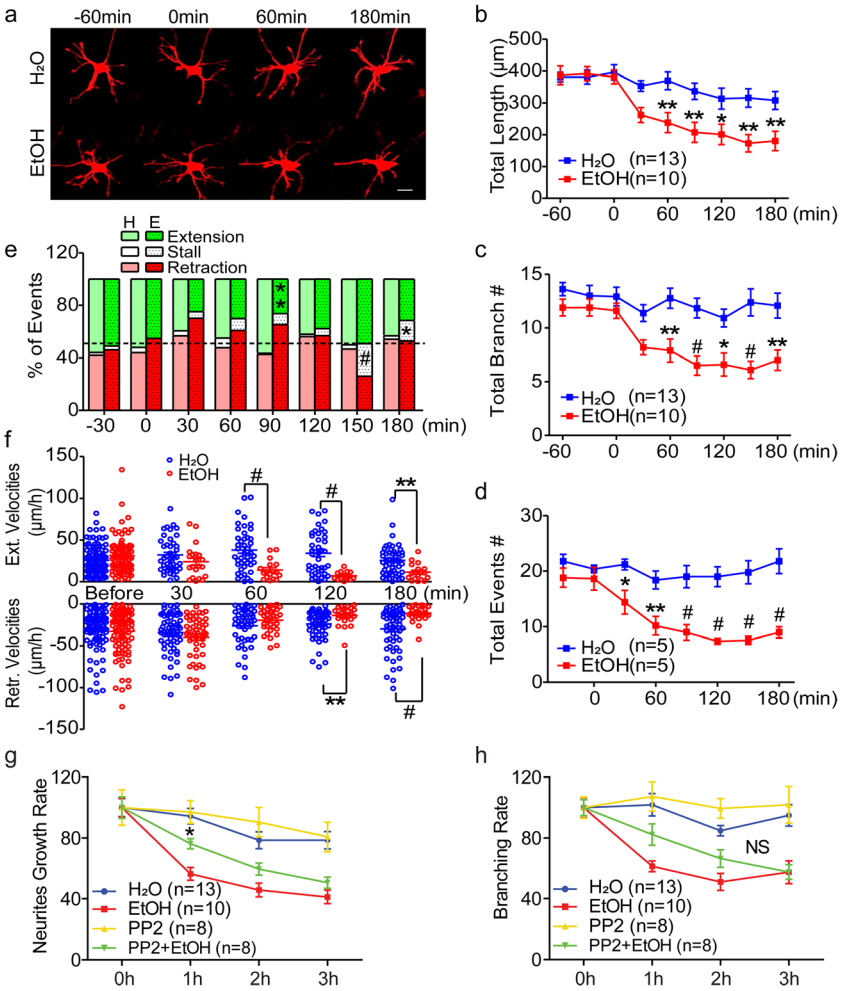

Fig. 3 Ethanol exposure impairs dendritic outgrowth. **a** Representative images of neurons from H_2O- and EtOH-treated cultures during a 4-h imaging period. The cells were transfected with Dcx-dsRed vector to visualize morphology. Scale bar = 10 μm. **b**–**c** Quantification of total dendrites length (**b**) and branch number (**c**) for neurons during a 4-h imaging period ($N_{H2O} = 13$, $N_{EtOH} = 10$). **d** Total neurite events (extension, retraction, and stall) per 30 min ($N_{H2O} = 5$, $N_{EtOH} = 5$). **e** Percentage of extension, stall, and retraction movements with H_2O or EtOH addition. **f** Quantitative analysis of neurite extension and retraction velocities before and after H_2O or EtOH exposure on a per neurite basis for each 30 min acquisition interval ($N_{H2O} = 5$, $N_{EtOH} = 5$). **g** PP2 transiently prevents EtOH-induced neurite growth impairment. **h** PP2 has no protective effect on neurite branching after EtOH exposure. Neurons were pre-incubated with PP2 (20 μM) 30 min prior to EtOH exposure. Two-way ANOVA followed by Bonferroni's multiple comparison test was performed between two groups and different time points. $^{*}p < 0.05$, $^{**}p < 0.01$, $^{\#}p < 0.001$

[38–42]. In addition, F-actin severed by cofilin can ultimately depolymerize to G-actin, increasing the pool of substrate for additional F-actin filament extension in new directions. As we observed a reduction in actin dynamics with an overall loss of arbor size, we sought to determine whether EtOH-exposure decreased cofilin activation as indicated by increased phosphorylation at Ser3 [43–45]. Surprisingly, levels of specific cofilin Ser3 phosphorylation were ~ 75% decreased in lysates derived from the culture 30 min after EtOH exposure ($EtOH_{30\ min} = 0.26 \pm 0.03$ vs. $H_2O = 1.0 \pm 0.3$, $^{**}p < 0.01$; Fig. 4a, b) and phosphorylation steadily declined by 93% by 4 h ($^{\#}p < 0.0001$; Fig. 4b) suggesting cofilin is strongly activated by EtOH. This cofilin activation is delayed by ~ 20 min from the phosphotyrosine response as shown in Fig. 1 ($EtOH_{10\ min} = 0.99 \pm 0.3$ vs. $H_2O = 1.0 \pm 0.33$, NS, $p > 0.05$; Fig. 4b) and is sustained for hours compared to the relatively transient phosphotyrosine response raising the possibility that alteration of cofilin activity is a contributor to EtOH-induced dendritic disruption.

To explore the specific consequences of EtOH exposure on F-actin distribution, we used AlexaFluor555-phalloidin to label F-actin and compared this signal to βIII-tubulin immunostaining that identifies microtubules. F-actin was mainly localized at the tips of neurites in neurons from the control (H_2O) group (Fig. 4c, e, arrow). However, in the presence of EtOH, the phalloidin signal was no longer concentrated at the tips, but rather was more diffuse along the whole neurite (Fig. 4d, f, arrow). The ratio of average F-actin density to tubulin in the distal neurite (5 μm from the tip) was significantly decreased in EtOH-treated neurons compared to control (EtOH = 3.47 ±

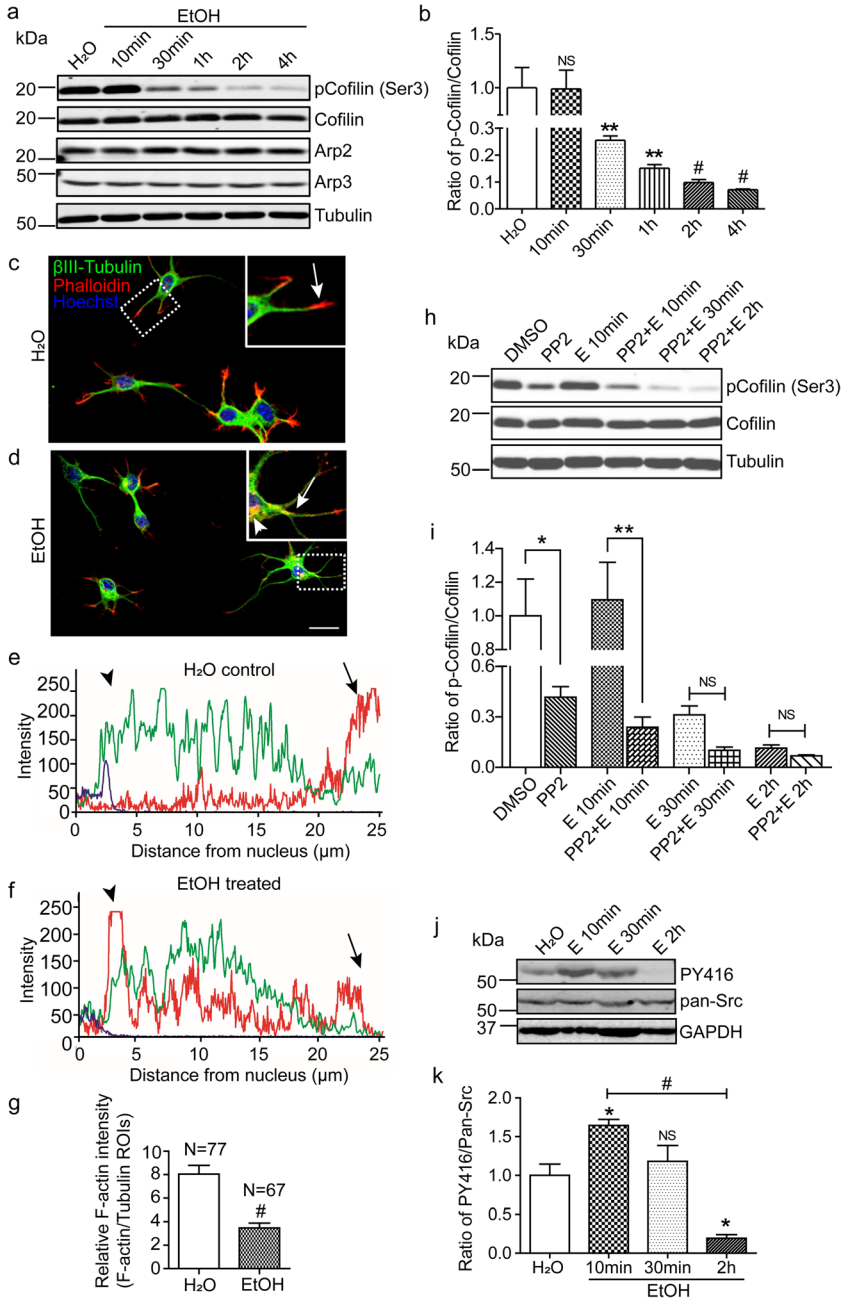

Fig. 4 Effects of ethanol on actin regulatory proteins. **a** The level of cofilin phosphorylation and Arp2/3 in E15 cortical culture was assayed after 0.5% EtOH exposure. Cortical culture lysates were probed with antibodies specific for the phosphorylated Ser3 residue of cofilin (top panel), cofilin, and Arp2/3. Blots were probed with anti-βIII tubulin as a loading control (bottom panel). **b** Quantification of LI-COR blots signals of cofilin from **a**. **c**–**d** Subcellular immunolocalization of βIII-tubulin (green) and filamentous actin (Alex555-phalloidin, red). F-actin is enriched at the tip of neurites from controls (inset) but is diffuse along the neurite after EtOH exposure. Scale bar, 20 μm. **e**–**f** Quantified profiles of βIII-tubulin (green) and F-actin signals (red) along neurites from H_2O- (**e**) and EtOH-treated groups (**f**). Arrow indicates the localization of F-actin at the tip of neurites in H_2O-treated neuron; arrowhead indicates the abnormal cluster of F-actin localized at the base of neurites in the presence of EtOH. **g** The ratio of F-actin versus tubulin signal at the distal neurite (5 μm from the tip) in H_2O- and EtOH-treated neurons. A total of 77 dendrites in H_2O group and 67 in EtOH group were quantified. **h**–**i** The level of cofilin phosphorylation was assayed after different time after EtOH exposure with or without PP2 preincubation. PP2 application by itself activated cofilin and PP2 preincubation did not protect neurons from EtOH-induced cofilin activation. **j**–**k**, A significant decrease of Src pY416 phosphorylation indicates Src is inactivated by longer term EtOH exposure. One-way ANOVA with Bonferroni post-hoc test was performed between different groups. $^{*}p < 0.05$, $^{**}p < 0.01$, $^{\#}p < 0.0001$, NS, $p > 0.05$

0.41 vs. $H_2O = 8.04 \pm 0.74$, $^{\#}p < 0.0001$, $N_{H2O} = 7$, $N_{EtOH} = 26$, Fig.4g). In addition, a subset of neurons from the EtOH group showed an increase in somatic F-actin signal with prominent perinuclear staining, indicative of a large scale

redistribution of F-actin within those cells (Fig. 4d, f arrow head). Together, these results demonstrate that EtOH exposure aberrantly dephosphorylates and activates cofilin, likely contributing to the observed redistribution of F-actin within the neuronal dendrite.

To determine whether PP2 could protect neurons from EtOH-induced cofilin activation, cortical cultures were treated with EtOH, with or without a 30 min preincubation of the SFK inhibitor PP2 (Fig. 4h, i). PP2 pretreatment did not protect neurons from dephosphorylation of cofilin at 30 min and 2 hr of EtOH exposure ($EtOH_{30\ min} = 0.31 \pm 0.05$ vs. PP2 + $EtOH_{30\ min} = 0.10 \pm 0.02$, $EtOH_{2h} = 0.11 \pm 0.02$ vs. PP2 + $EtOH_{2h} = 0.07 \pm 0.01$, NS, $p > 0.05$). Surprisingly, PP2 treatment alone induce dephosphorylation of cofilin (PP2 = 0.42 ± 0.11 vs. DMSO = 1.0 ± 0.38, $^{*}p < 0.05$), which suggests that Src inhibition is sufficient to activate cofilin in these neuronal cultures. To determine Src activation status at 30 min and 2 hr after EtOH exposure, lysates were probed for pY416 SFK activation loop levels. In contrast to the Src activation observed at 10 min EtOH exposure (Fig. 1e), a trend towards declining Src activation was detected by 30 min of EtOH exposure, which is significant after 2 h of exposure ($EtOH_{2\ h} = 0.19 \pm 0.08$ vs. $H_2O = 1.0 \pm 0.25$, $^{*}p < 0.05$; $EtOH_{2h} = 0.19 \pm 0.08$ vs. $EtOH_{10\ min} = 1.64 \pm 0.14$, $^{\#}p < 0.001$, Fig. 4j–k). Together, these data indicate that EtOH-exposure initially (10 min) activates but then inactivates Src (≥ 30 min) and the sustained Src inactivation may contribute to cofilin activation.

Sustained Impairment of Reelin-Dab1 Signaling by Ethanol

Although the initial (~ 10 min) biochemical events stimulated by EtOH are similar to the events stimulated by Reelin-signaling (e.g., Src activation and Dab1 phosphorylation), the later (> 30 min) effects including Src inactivation, cofilin dephosphorylation, and slower neurite dynamics are different [9, 37]. Therefore, to determine whether Reelin signaling is abrogated at > 30 min after EtOH exposure, we first exposed cultured neurons to EtOH for 30 min and then attempted to stimulate Reelin signaling by applying recombinant Reelin. While control (H_2O-treated) cultures showed Dab1 tyrosine phosphorylation in response to 20 min of applied Reelin (Fig. 5a), the EtOH-treated cultures showed little or no Dab1 response after EtOH-pretreatment (Fig. 5b). In addition, Reelin application had no effect on the EtOH-induced activation of cofilin indicated by the unchecked decline in cofilin Ser3 phosphorylation ($EtOH_{30\ min}$ w/Reelin = 0.1 ± 0.02 vs. $EtOH_{30\ min} = 0.26 \pm 0.05$, NS, $p > 0.05$; $EtOH_{2\ h}$ w/Reelin = 0.07 ± 0.02 vs. $H_2O = 1.0 \pm 0.14$, $^{**}p < 0.01$; $EtOH_{4\ h}$ w/Reelin = 0.05 ± 0.01 vs. $H_2O = 1.0 \pm 0.14$, $^{**}p < 0.01$; Fig. 5c–d). Given the observed long-term Src inactivation (Fig. 4j, k) by EtOH, these findings indicate that 30 min after

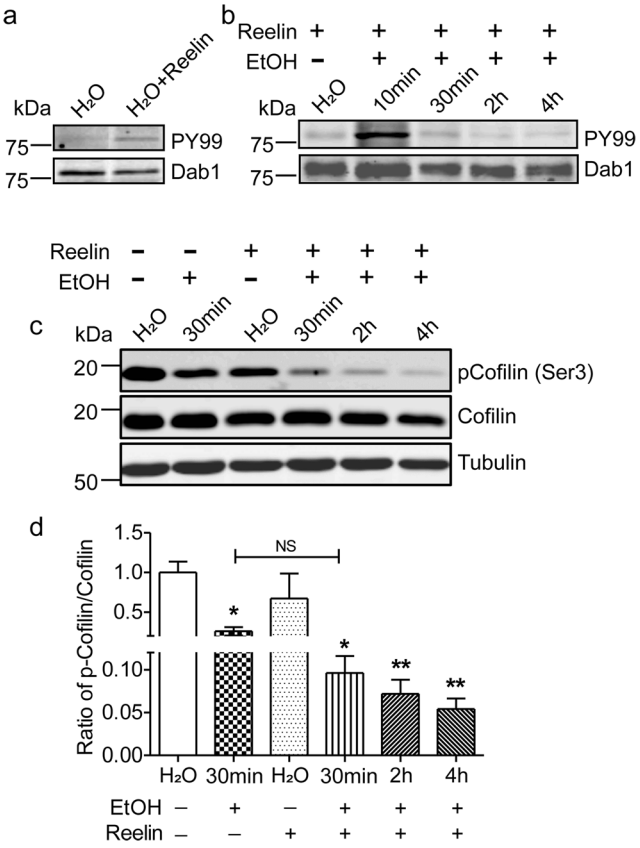

Fig. 5 Ethanol exposure renders neurons insensitive to Reelin. **a** Reelin-conditioned medium (RM) application for 20 min enhanced the Dab1 phosphorylation in H_2O-pretreated control cultures. **b**–**c** In contrast, RM application did not stimulate Dab1 phosphorylation (**b**) or cofilin Ser3 phosphorylation (**c**) 30 min after 0.5% EtOH exposure. Anti-βIII tubulin was used as a loading control. **d** Quantification of blots from **c**. One-way ANOVA followed by Bonferroni post hoc test was used between different groups. $^{*}p < 0.05$, $^{**}p < 0.01$

EtOH exposure, the neuron is rendered insensitive to applied Reelin because SFKs cannot be activated.

In Vivo Elevation of Tyrosine Phosphorylation and Disrupted Dendritogenesis After Ethanol Exposure

To determine whether rapid EtOH-induced tyrosine phosphorylation occurs in vivo, pregnant dams received an i.p. injection of EtOH (400 mg/dL) or PBS on E15. The dams were euthanized; the embryos were removed, and the embryonic dorsal neocortex was dissected approximately 10 min and 30 min after injection. Lysates were generated, and western blots performed for the detection of tyrosine-phosphorylated protein. Consistent with the cell culture results (Fig. 1), EtOH injection caused a rapid ~ 4 fold elevation of tyrosine phosphorylation lysates from the dorsal cortex compared to lysates prepared from controls at 10 min (1.0 ± 0.1 in H_2O vs. 3.5 ± 0.4 in EtOH, $^{\#}p < 0.0001$; Fig. 6a, b), but increased tyrosine phosphorylation was not observed in embryos from dams that

had been injected 30 mins prior (Fig. 6c, d). Additionally, EtOH exposure produced similar enhancement of tyrosine phosphorylation in whole hemisphere explants, establishing the validity of an explant approach for examining these phenomena (see below and Fig. 7a). This finding indicates that acute exposure to EtOH likely triggers a similar biochemical cascade in vivo as observed in vitro.

To determine whether acute EtOH exposure alters the growth and branching of the apical dendrite in its native context, we performed multiphoton imaging of embryonic whole hemisphere explants. Neural precursors were labeled with pCAG-tdTomato plasmid by ex utero electroporation at E13 and whole hemisphere explants were prepared [9, 46]. After 2 DIV, to allow for neurogenesis, multiphoton imaging was performed on developing deep layer neurons soon after they completed migration. Z-series were captured every 10 min over a 5-h period. An initial 1-h baseline period was followed by continuous application of 0.5% EtOH for an additional 4 h. Similarly, prepared control explants were imaged with an equivalent volume of applied H_2O (N=10 in H_2O and EtOH group individually). Neurons with their somas located 50 μm of the pial surface were selected for quantification. For control neurons in the H_2O group, the total apical neurites increased ~ 150% in size ($H_2O_{-1\ h} = 147.8 \pm 11.8$ vs. $H_2O_{4\ h} = 241.7 \pm 21$; Fig. 7c) with increased branching number and complexity during the 5-h imaging period (Fig. 7d). However, following EtOH exposure, there was a rapid arrest of dendritic growth followed by a slower ~ 30% reduction of arbor size ($EtOH_{-1\ h} = 175.7 \pm 1.0$; $EtOH_{4\ h} = 124.4 \pm 11.7$ vs. $H_2O_{4\ h} = 241.7 \pm 21$, $^{\#}p < 0.001$; Fig. 7c) and a 20% decrease in branch number ($EtOH_{-1\ h} = 7.4 \pm 0.5$; $EtOH_{4\ h} = 6.1 \pm 0.5$ vs. $H_2O_{4\ h} = 10.2 \pm 1.0$, $^{**}p < 0.01$; Fig. 7d). As shown in Fig. 7e, the total dendritic movements gradually decreased after EtOH exposure. Also, there was a significant decrease of extension events at 30 min that continued with EtOH exposure compared with H_2O-treated dendrites ($EtOH_{30\ min} = 23.5\% \pm 10.3\%$ vs. $H_2O_{30\ min} = 63.6\% \pm 7.1\%$, $^{**}p < 0.01$; Fig. 7f). After quantification of event velocities, EtOH induced an increased retraction speed 30-min postexposure which caused the rapid collapse of apical dendrites even though there is no difference at later time points ($EtOH_{30\ min} = 21.1 \pm 2.6$ vs. $H_2O_{30\ min} = 10.4 \pm 1.8$, $^{*}p < 0.05$; Fig. 7g). Thus, the dendritic response to EtOH exposure in organotypic explants was similar to the dendritic responses in dissociated cell culture with a rapid onset of altered neurite growth and branching, and reduced extension and retraction events.

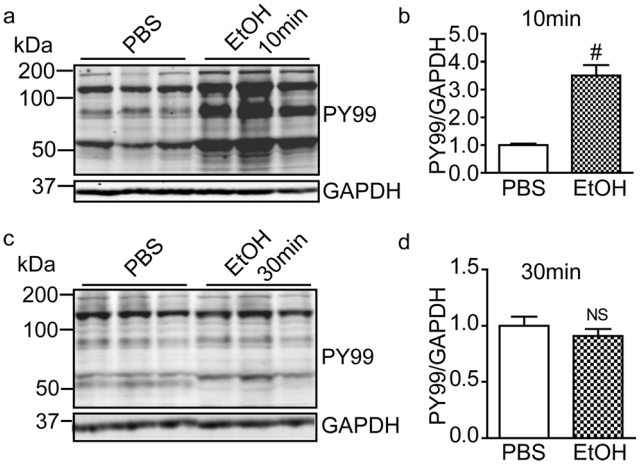

Fig. 6 Transient increase in tyrosine phosphorylation after ethanol exposure in vivo. **a** I.P. injection of EtOH (4 g EtOH/kg bodyweight, equivalent to 0.5%, *v/v*) into the pregnant dam induced an increased tyrosine phosphorylation detected in lysates (lysates prepared ~ 10 min after injection) from embryonic cortex. **c** Increased tyrosine phosphorylation was not detected 30 min after EtOH injection. **b**, **d** Quantification of blots from **a** and **c** respectively. Student's *t* test was used between two groups. $^{\#}p < 0.0001$, NS, $p > 0.05$

The apical dendrite emerges by direct transformation of the leading process of the migrating cortical neuron [9, 26]. Thus, the end stage of migration, called translocation [47] and dendritic initiation are coincident, and it has been proposed that they are mechanistically coupled processes [9, 48, 49]. To assess the migration behavior after EtOH exposure, we quantified the somal movement of those translocating neurons. Based on our previous studies [9, 50], we focused on translocating neurons that had somas located between 80 and 50 μm below the pia but with leading processes that were within 15 μm of the pial surface (i.e., within the marginal zone) at the beginning of the imaging period. We compared migratory speeds in control (H_2O) and EtOH-treated explants. The speed of migration was statistically compared by binning the 0–2 h and 2–4 h postexposure periods. Contrary to expectations, neurons in both groups successfully translocated with no difference in their translocating speed during either exposure epoch (t_{0h} 35.0 ± 2.3 in H_2O vs. 31.4 ± 3.7 in EtOH; t_{2h} 32.2 ± 2.9 in H_2O vs. 40.1 ± 3.6 in EtOH, $p > 0.05$; Fig. 7h–j). Thus, dendritogenesis is disrupted by EtOH exposure but terminal translocation is unaffected.

Discussion

In this study, we identified a dramatic and rapid increase in SFK-dependent tyrosine phosphorylation after EtOH exposure. This increased phosphorylation occurred on multiple proteins and was temporally correlated with disruption of apical dendrite growth. Three lines of evidence indicate that EtOH activates SFKs: first, the EtOH response is almost entirely blocked by PP2 and SKI-1, selective inhibitor of SFKs, but not the Abl kinase inhibitor, imatinib. Second, we demonstrated increased phosphorylation on pY416 of the Src activation loop. Third, we demonstrated increased tyrosine phosphorylation of Dab1, a well characterized substrate of SFKs. The mechanism underlying this activation is presently unclear. In corticostriatal cultures, EtOH specifically activates Fyn but

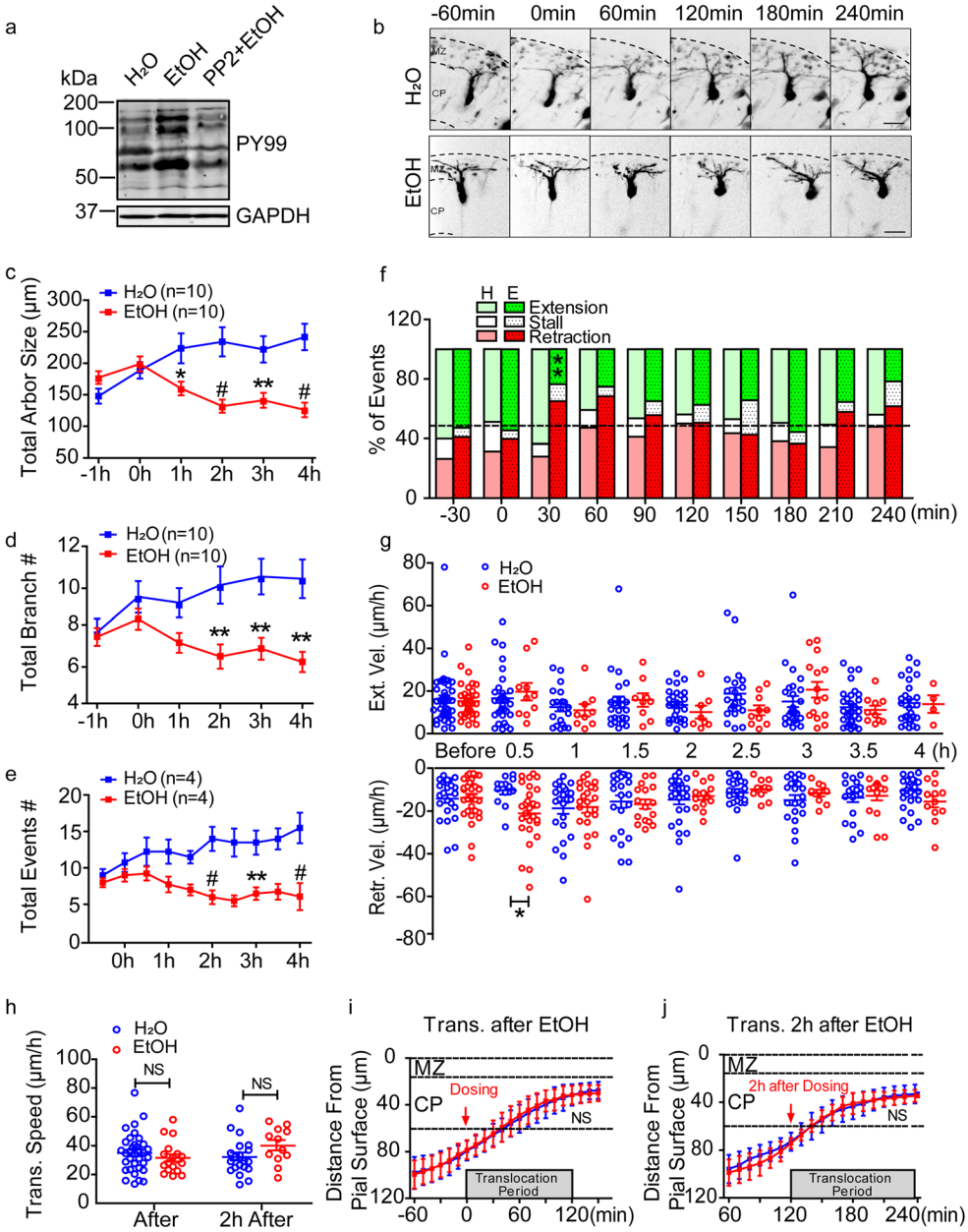

Fig. 7 Ethanol disrupts dendritogenesis but not somal translocation. **a** 10 min of EtOH (0.5%, *v*/*v*) induced an elevation of tyrosine phosphorylation, which could be blocked by 20 μM PP2 in E15 explants. **b** Multiphoton images of tdTomato-labeled deep layer neurons during the early period apical dendrite growth. Whole hemisphere explants were imaged at 10 min of intervals for a period of 5 h, with 1-h baseline followed by 4-h treatment of H_2O (control) or EtOH (0.5%). **c**–**d** Quantification of arbor size (**c**) and branch number (**d**) of tdTomato + neurons during EtOH (400 mg/dL, 0.5%, *v*/*v*) exposure compared with control neurons (N = 10). Control neurons displayed larger arbors with more branch number over time, whereas EtOH-treated neurons showed a rapid collapse and reduction of branch number. **e** Total neurite extension, stall, and retraction events per 30 min ($N_{H2O} = 4$, $N_{EtOH} = 4$). **f** Percentage of extension, stall, and retraction movements with H_2O or EtOH addition. **g** Quantitative analysis of neurite extension and retraction velocities before and after H_2O or EtOH exposure on a per neurite basis for each 30-min acquisition interval ($N_{H2O} = 4$, $N_{EtOH} = 4$). **h** Translocation speed of migrating neurons in the presence of EtOH was compared with H_2O by binning 0–2 and 2–4 h postexposure values. **i**–**j**, Quantification of somal positioning and translocation speed immediately after exposure (**i** $N_{H2O} = 34$, $N_{EtOH} = 18$) or 2 h later (**j** $N_{H2O} = 20$, $N_{EtOH} = 12$). Neurons after H_2O and EtOH exposure demonstrated similar translocation characteristic. Two-way ANOVA followed by Bonferroni's multiple comparison tests were performed between two groups and different time points. $^{*}p < 0.05$, $^{**}p < 0.01$, $^{\#}p < 0.001$, NS, $p > 0.05$. Scale bars in **b**, 20 μm

not Src via protein tyrosine phosphatase alpha (PTPα)-mediated dephosphorylation of Fyn at Y527 [51]. However, in our embryonic cortical culture model, we did not observe a significant increase in Fyn activation. Also, we find robust activation of tyrosine kinase activity in the presence of PAO which should largely block PTPα activity. This suggests that a

distinct mechanism can function in embryonic cortical neurons to activate Src. In addition, we do not know whether all of the proteins that demonstrate increased pY content after EtOH exposure are direct SFKs substrates or substrates of an unidentified tyrosine kinase that is activated by SFKs [52, 53]. While the mechanism underlying the activation of SFKs is unknown, the transient increase in phosphotyrosine content after EtOH exposure is followed by the sustained blunting of Reelin/Src/Dab1-signaling and the sustained activation of cofilin. It is likely that these sustained signaling disruptions produced by EtOH contribute to the long-term disruptions of dendritogenesis.

The Reelin signaling pathway plays a critical role in dendrite stabilization via activation of SFKs. Reelin, secreted by Cajal-Retzius neurons in the marginal zone of the developing cortex, binds low density lipoprotein receptor family members expressed by the underlying differentiating cortical neuron. This binding clusters the receptors and activates two SFKs, Src and Fyn, which in turn, phosphorylate the cytoplasmic adaptor protein Dab1. Phospho-Dab1 then functions as a critical hub in a signaling pathway that triggers multiple downstream effects including phosphorylation and inactivation of n-cofilin [54] to effect cytoskeletal stabilization. Importantly, studies involving PP2 treatment of cortical slice cultures [55] or examination of mice doubly deficient of the SFKs Src and Fyn [56] revealed cortical disruptions that are very similar to those found in reeler cortices, namely disrupted preplate splitting and aberrant neuronal morphology. This close phenocopy identifies a primary role for Src and Fyn during this early period of brain development. Thus, any action that disrupts SFKs function during early cortical development is expected to disrupt Reelin signaling.

Our prior study explored the effects of EtOH on early stages of apical dendrite initiation and growth. Using an organotypic whole hemisphere explant model, we found that cortical neurons exposed to EtOH showed similar, albeit less severe morphological disruptions as neurons in Reelin-deficient (reeler) explants with simplified and stunted dendritic arbors, more compact Golgi apparatus and altered MAP 2 immunohistochemical signals [16, 17]. The similarity in phenotypes between reeler neurons and EtOH-exposed neurons raised the possibility that EtOH directly interfered with Reelin-signaling. Surprisingly, biochemical analysis suggests the opposite: acute EtOH exposure dramatically activated SFKs signaling, leading to the tyrosine phosphorylation of multiple proteins including Dab1 suggesting that EtOH activates initial events in Reelin signaling. However, there are some immediate distinctions between EtOH dependent activation and Reelin-dependent activation: first, Reelin-dependent activation is fairly selective for Src kinase and Dab1 [57]. In contrast, EtOH activation targets multiple proteins. Second, Reelin dependent activation is more sustained, with evidence of sustained pY on Dab1 for hours, whereas EtOH induced a transient pY elevation but persistent silence including Src tyrosine kinase after 30 min. Finally, Reelin signaling leads to Dab1 phosphorylation and ultimately Dab1 degradation [58] whereas we did not reliably detect Dab1 downregulation after EtOH exposure (data not shown). Similarly, there are also important differences in the cellular phenotypes between EtOH exposure and Reelin-signaling deficiency after analyses of neurite kinetics: dendritic filopodia both extend and retract faster in reeler than in wildtype cortices [9]. Using organotypic explants, we did not detect a difference in neurite extension and retraction velocities after EtOH-exposure while in culture, we find the opposite, with EtOH-exposed dendrites showing reduction in both extension and retraction velocities within 30 min of exposure. The variation here might be due to differing substrates for neurite growth, poly-D-lysine for cultured neurons versus neuronal extracellular matrix and cellular elements in the explants [59, 60]. Thus, EtOH-exposure, interferes with Reelin-Dab1 signaling but also disrupts dendritic growth by other mechanism(s). The existence of additional pathway(s) mediating dendritic collapse besides SFKs activation was confirmed by PP2 pretreatment study which ultimately could not protect dendritic collapse caused by EtOH exposure (Fig. 3g, h).

Prior findings have identified disruptions of F-actin after EtOH exposure. In cerebellar cells, F-actin filaments are rapidly depolymerized as a consequence of 30 sec of 100 mM ethanol exposure [61]. Moreover, a reduction in F-actin content is observed in cultured hippocampal neurons after prolonged (14 days) EtOH-exposure, without changes in total actin [62, 63]. In our study, EtOH exposure is associated with dephosphorylated (Ser3) and activated cofilin, a critical F-actin severing protein. This activation of cofilin can be produced PP2 treatment alone (Fig. 4h–i) underscoring the link between EtOH-induced Src inactivation and cofilin activation. Although cofilin-dependent severing of F-actin might lead to neurite retraction, the situation is likely more complicated, and it is clear that cofilin-dependent F-actin severing is essential for F-actin dynamics and neurite outgrowth as well [38]. Thus, our finding of dephosphorylated cofilin might have been expected to be correlated with enhanced neurite dynamics rather than reduced. However, the observed redistribution of F-actin away from the neurite tips and towards the soma would be more consistent with increased retrograde F-actin flow. This apparent mismatch between cofilin activation and F-actin distribution after EtOH exposure might be accounted for by interference of other actin-regulatory proteins, possibly profilin or Arp2/3 as well as additional signaling events triggered by EtOH exposure. One possibility is that 10 min of EtOH abnormally activated ADF/cofilin and enhanced F-actin severing, but also impaired the protrusion of microtubules that is required for neurite extension [12, 62]. In addition, EtOH exposure can disrupt actin dynamics in ways that do not involve ADF/cofilin [63, 64]. While the mechanistic

understanding of EtOH-dependent kinase activation and dendritic damage are incomplete, the long-term Src inactivation is a likely important contributor to the neurodevelopmental disruptions caused by fetal alcohol exposure.

Experimental Procedures

Mice

Animals were used in compliance with approved protocols by the Institutional Animal Care and Use Committee of SUNY Upstate Medical University. Timed pregnant Swiss Webster dams were purchased from Charles River Laboratories (Wilmington, MA, USA). The day of plug discovery is considered embryonic day 0 (E0).

Cortical Cultures and Treatments

Cultured cortical neurons were obtained from either E15 explants (2 DIV after E13 electroporation) or E15 embryos. Cortical neurons were dissociated using 0.25% Trypsin at 37 °C for 20 min. 10:10 buffer (10% trypsin inhibitor and 10% Bovine Serum Albumin, both from Sigma) was used to neutralize Trypsin. Neurons were resuspended in Neurobasal medium supplemented with 2% B27, 1% GlutaMAX, and 1% penicillin/streptomycin (all from Invitrogen) and plated on poly-D-lysine (PDL)-coated dishes with a glass bottom (MatTek Corporation) at a final concentration of 2×10^5 cells/ml for confocal live imaging or cultured in 24-well plates with PDL-coated glass coverslips for immunohistochemistry. For western blot and immunoprecipitation, cortical cultures were plated on PDL-coated 6-well tissue culture plates at a final concentration of 2×10^6 cells/ml and cultured for another 72 h.

For confocal live imaging, cultured embryonic neurons were identified by Dcx-dsRed fluorescence [65] (gift of Dr. Q. Lu, City of Hope) after electroporation on E13. High-resolution images were acquired with a Zeiss LSM 780 laser scanning confocal microscope using a Plan-Apochromat 40x/1.4 NA objective. The dendritic outgrowth of individual neurons was recorded at a 10 min interval for both the 1 h baseline and 3 h of EtOH exposure, with or without PP2 pretreatment (20 μM, 30 min).

For western blotting and immunoprecipitation experiment, E15 cortical neurons were treated with EtOH (400 mg/dL, 0.5% *v*/*v*) for different durations or different concentrations of EtOH (0.125%, 0.25%, 0.5%, 0.75%, *v*/*v*) for 10 min in the presence or absence of 20 μM PP2 (Bio-Techne Corporation, Minneapolis, MN, USA), 100 nM imatinib (Sigma), 1 μM STI-571 (Sigma), 20 μM phenylarsine oxide (PAO) (Sigma), 500 μM cholesterol (Sigma), 500 μM Methyl-β-Cyclodextrins (MβCDs, Sigma), or Reelin condition medium in separate experiments. PP2, imatinib PAO, cholesterol, or MβCD were added 30 min (also 40 min or 60 min for PAO) prior to EtOH treatment. STI-571 was added 1 h before EtOH exposure. Reelin medium was applied 20 min after ethanol exposure.

Immunohistochemistry

E15 cortical neurons grown on glass coverslips were fixed with 4% paraformaldehyde for 15 min after ethanol exposure on DIV 3. Cells were blocked with 5% BSA and 0.2% TritonX-100 for 1 h at room temperature and incubated with mouse anti-Tuj1 antibody (1:1000, Promega) at 4 °C overnight, followed by AlexaFluor 488-conjugated secondary antibodies and AlexaFluor 555-conjugated phalloidin (1:500, Invitrogen) for 1 h at room temperature. Hoechst 33342 (2 μg/ml, Molecular Probes) was used to visualize individual cell nuclei. Images were collected with a Zeiss LSM780 laser scanning confocal microscope (Confocal and Two-Photon Imaging Core, SUNY Upstate Medical University). The average F-actin signal density at distal neurite (5 μm from the tip) was normalized to the tubulin immunosignal intensity and compared between H_2O and EtOH-treated group.

Purification of Reelin-Conditioned Medium

Reelin-conditioned media was produced by a stable HEK293 cell line (gift of E. Förster, Universität Bochum) after 48 h of incubation in serum-free Opti-MEM media as described previously [9]. Amicon Ultra 100,000 molecular weight cut off filters (Millipore) were used to concentrate the conditioned media to 10-fold concentration and applied to the neuron culture media at a 5-fold final dilution.

Immunoprecipitation and Western Blot Analysis

E15 embryonic dorsal cortex, explants, and primary cortical neuron lysates were collected in radio immunoprecipitation assay (RIPA) buffer (50 mM Tris-HCl; 1% NP-40; 0.25% Na-Deoxycholate; 150 mM NaCl; 1 mM EDTA; pH 7.4) with protease inhibitors (P8340 Protease Inhibitor Cocktail, Sigma) and phosphatase inhibitors (1 mM Na_3VO_4; 1 mM NaF) on DIV 3. For immunoprecipitation assay, the lysates from cortical cultures were incubated with anti-Dab1 rabbit antibodies (3 μg/100 μl, Sigma), anti-pan Src mouse antibody (3 μg/100 μl, Millipore) or anti-Fyn rabbit antibody (1:40, Abcam) at 4 °C overnight, and precipitated with protein A/G-agarose beads (Santa Cruz Biology) for 2 h at 4 °C. For western blotting, all samples were loaded onto 10% SDS-PAGE gels and transferred to 0.45-μm PVDF Immobilon®-FL membranes (EMD Millipore). After incubation with Odyssey blocking buffer (LI-COR Biosciences) for 1 h at room temperature, the membranes were incubated with the following primary antibodies overnight at 4 °C. The primary antibodies were anti-pY99

(1:1000, SantaCruz), anti-Dab1 antibodies (1:1000, Sigma), anti-PY416 (1:1000, Cell Signaling), anti-pan Src antibody (1:1000, Millipore), anti-Fyn antibody (1:1000, Abcam), anti-phospho-Cofilin (Ser3) (1:200, SantaCruz), anti-Cofilin (1:200, SantaCruz), anti-Arp2 (1:200, SantaCruz), and anti-Arp3 (1:200, SantaCruz). Anti-GAPDH (1:2000, UBPBio) and anti-β tubulin (1:2000, Promega) were used as loading controls. Appropriate secondary antibodies IRDye® 800CW and IRDye® 680RD (LI-COR Biosciences) were used and membranes were scanned using ODYSSEY system (Odyssey® CLx, LI-COR Biosciences).

Ex Utero Electroporation and Explant Cultures

A whole hemisphere explant model was utilized in which organotypic development is observed for a period of 2 days in vitro (DIV) encompassing a period of preplate splitting and cortical layer formation, both Reelin-signaling dependent events [66, 67]. Explant preparation and ex utero electroporation were performed on day 13 embryos (E13) using 0.6 mg/ml of pCAG-TdTomato [9] or 0.8 mg/ml of Dcx-dsRed construct [65]. Hemispheres were dissected and cultured medial side down on 3-μm pore size collagen-coated polytetrafluoroethylene filters (Transwell-COL; Corning) in DMEM-F12 medium plus GlutaMAX and supplemented with 1% G5, 2% B27, and 1% penicillin/streptomycin and maintained in a high oxygen environment (95/5% O_2/CO_2) at 37 °C for 48 h before two-photon imaging or cortical culture. All cell culture reagents were from Invitrogen.

Two-Photon Live Imaging

Explants electroporated with pCAG-tdTomato (0.6 mg/ml) were imaged while under continuous perfusion with oxygenated medium (DMEM-F12 and 20 μM HEPES) warmed by a SH7B inline heater (Warner Instruments). Four milligrams per deciliter (0.5%, *v*/*v*) ethanol or equivalent volumes of H_2O were added into the perfusion medium after 1 h of baseline was collected. Imaging was performed as described previously [9] by using a ThorA multiphoton microscope (Thorlabs) coupled to an Insight DeepSee Multiphoton Ti:Sapphire tunable laser (Spectra-Physics). Images were collected with an Olympus × 20/1.0 NA water-immersion objective with a 2-mm working distance. A wavelength of 910 nm was used for the tdTomato signal. Z-series were acquired every 10 min for up to 4 h at 1-μm z-intervals. A total of ten neurons in H_2O or EtOH group from > 3 different experiments were analyzed.

Image Analysis

Two photon z-series were imported into FIJI for concatenation and registration. Individual neurons were traced at all time points using the Simple Neurite Tracer plugin within Fiji. Distance below the pial surface, total apical arbor size, and total apical branch number were measured at each time point from the registered and hyperstacked traces. For translocating speed analysis, only well isolated cells with soma between 80 and 50 μm below the pial and with leading process that contacted the marginal zone during the first hour of the imaging period were analyzed. To analyze neurite dynamics in cortical cultures, confocal images were also imported into FIJI, traced using the Simple Neurite Tracer plugin and neurite extension, and retraction velocities were determined on a per neurite basis for each 30-min period.

Statistical Analysis

Data are presented as the mean ± SEM. Differences between groups were assessed using Student's *t* test. For neurite morphology measurement and dose/time response in EtOH exposure experiment, one- or two-way ANOVA with post-hoc Bonferroni tests was used. The results were averaged from multiple experiments. Statistical significance was determined when $p < 0.05$.

Acknowledgements We thank members of the Olson lab and Krysten O'Hara for assistance and valuable input on the project.

Author Contribution EO and DW designed the study with significant input from BH. DW and JE performed the study. EO and DW wrote the manuscript with comments and edits from BH, JE, and members of the Developmental Exposure to Alcohol Research Center (DEARC).

Funding Information This work was supported by the National Institute on Alcohol Abuse and Alcoholism (NIAAA) via the Developmental Exposure to Alcohol Research Center (DEARC) P50AA017823-10.

Compliance with Ethical Standards

Conflict of Interest The authors declare that they have no competing interests.

Abbreviations FASD, fetal alcohol spectrum disorder; SFKs, Src family kinases; EtOH, ethanol; PAO, phenylarsine oxide; MβCDs, methyl-β-cyclodextrins; RM, Reelin-conditioned medium

References

1. May PA, Chambers CD, Kalberg WO, Zellner J, Feldman H, Buckley D, Kopald D, Hasken JM et al (2018) Prevalence of Fetal Alcohol Spectrum Disorders in 4 US Communities. JAMA 319:474–482
2. Kodituwakku PW, Handmaker NS, Cutler SK, Weathersby EK, Handmaker SD (1995) Specific impairments in self-regulation in children exposed to alcohol prenatally. Alcohol Clin Exp Res 19: 1558–1564

3. Mattson SN, Riley EP (1998) A review of the neurobehavioral deficits in children with fetal alcohol syndrome or prenatal exposure to alcohol. Alcohol Clin Exp Res 22:279–294
4. Rodriguez CI, Davies S, Calhoun V, Savage DD, Hamilton DA (2016) Moderate prenatal alcohol exposure alters functional connectivity in the adult rat brain. Alcohol Clin Exp Res 40:2134–2146
5. Ishii S, Hashimoto-Torii K (2015) Impact of prenatal environmental stress on cortical development. Front Cell Neurosci 9:207
6. Yanni PA, Lindsley TA (2000) Ethanol inhibits development of dendrites and synapses in rat hippocampal pyramidal neuron cultures. Brain Res Dev Brain Res 120:233–243
7. Lindsley TA, Mazurkiewicz JE (2013) Ethanol modulates spontaneous calcium waves in axonal growth cones in vitro. Brain Sci 3: 615–626
8. Servais L, Hourez R, Bearzatto B, Gall D, Schiffmann SN, Cheron G (2007) Purkinje cell dysfunction and alteration of long-term synaptic plasticity in fetal alcohol syndrome. Proc Natl Acad Sci U S A 104:9858–9863
9. O'Dell RS, Cameron DA, Zipfel WR, Olson EC (2015) Reelin prevents apical neurite retraction during terminal translocation and dendrite initiation. J Neurosci 35:10659–10674
10. Picken Bahrey HL, Moody WJ (2003) Early development of voltage-gated ion currents and firing properties in neurons of the mouse cerebral cortex. J Neurophysiol 89:1761–1773
11. Cameron DA, Middleton FA, Chenn A, Olson EC (2012) Hierarchical clustering of gene expression patterns in the Eomes + lineage of excitatory neurons during early neocortical development. BMC Neurosci 13:90
12. Guadagnoli T, Caltana L, Vacotto M, Gironacci MM, Brusco A (2016) Direct effects of ethanol on neuronal differentiation: an in vitro analysis of viability and morphology. Brain Res Bull 127: 177–186
13. Goeke CM, Roberts ML, Hashimoto JG, Finn DA, Guizzetti M (2018) Neonatal ethanol and choline treatments alter the morphology of developing rat hippocampal pyramidal neurons in opposite directions. Neuroscience 374:13–24
14. Fontaine CJ, Patten AR, Sickmann HM, Helfer JL, Christie BR (2016) Effects of pre-natal alcohol exposure on hippocampal synaptic plasticity: sex, age and methodological considerations. Neurosci Biobehav Rev 64:12–34
15. Louth EL, Luctkar HD, Heney KA, Bailey CDC (2018) Developmental ethanol exposure alters the morphology of mouse prefrontal neurons in a layer-specific manner. Brain Res 1678:94–105
16. Powrozek TA, Olson EC (2012) Ethanol-induced disruption of Golgi apparatus morphology, primary neurite number and cellular orientation in developing cortical neurons. Alcohol 46:619–627
17. O'Dell RS, Ustine CJ, Cameron DA, Lawless SM, Williams RM, Zipfel WR, Olson EC (2012) Layer 6 cortical neurons require Reelin-Dab1 signaling for cellular orientation, Golgi deployment, and directed neurite growth into the marginal zone. Neural Dev 7: 25
18. Jossin Y, Cooper JA (2011) Reelin, Rap1 and N-cadherin orient the migration of multipolar neurons in the developing neocortex. Nat Neurosci 14:697–703
19. Jossin Y, Goffinet AM (2007) Reelin signals through phosphatidylinositol 3-kinase and Akt to control cortical development and through mTor to regulate dendritic growth. Mol Cell Biol 27: 7113–7124
20. Kuo G, Arnaud L, Kronstad-O'Brien P, Cooper JA (2005) Absence of Fyn and Src causes a reeler-like phenotype. J Neurosci 25:8578–8586
21. La Torre A, del Mar Masdeu M, Cotrufo T, Moubarak RS, del Rio JA, Comella JX, Soriano E, Urena JM (2013) A role for the tyrosine kinase ACK1 in neurotrophin signaling and neuronal extension and branching. Cell Death Dis 4:e602
22. Finsterwald C, Fiumelli H, Cardinaux JR, Martin JL (2010) Regulation of dendritic development by BDNF requires activation of CRTC1 by glutamate. J Biol Chem 285:28587–28595
23. Qiu S, Lu Z, Levitt P (2014) MET receptor tyrosine kinase controls dendritic complexity, spine morphogenesis, and glutamatergic synapse maturation in the hippocampus. J Neurosci 34:16166–16179
24. Oliva C, Hassan BA (2017) Receptor tyrosine kinases and phosphatases in neuronal wiring: insights from drosophila. Curr Top Dev Biol 123:399–432
25. D'Arcangelo G, Miao GG, Chen SC, Soares HD, Morgan JI, Curran T (1995) A protein related to extracellular matrix proteins deleted in the mouse mutant reeler. Nature 374:719–723
26. Pinto-Lord MC, Evrard P, Caviness VS Jr (1982) Obstructed neuronal migration along radial glial fibers in the neocortex of the reeler mouse: a Golgi-EM analysis. Brain Res 256:379–393
27. Olson EC, Kim S, Walsh CA (2006) Impaired neuronal positioning and dendritogenesis in the neocortex after cell-autonomous Dab1 suppression. J Neurosci 26:1767–1775
28. Bock HH, Herz J (2003) Reelin activates SRC family tyrosine kinases in neurons. Curr Biol 13:18–26
29. Howell BW, Herrick TM, Hildebrand JD, Zhang Y, Cooper JA (2000) Dab1 tyrosine phosphorylation sites relay positional signals during mouse brain development. Curr Biol 10:877–885
30. Hanke JH, Gardner JP, Dow RL, Changelian PS, Brissette WH, Weringer EJ, Pollok BA, Connelly PA (1996) Discovery of a novel, potent, and Src family-selective tyrosine kinase inhibitor. Study of Lck- and FynT-dependent T cell activation. J Biol Chem 271:695–701
31. Oetken C, von Willebrand M, Marie-Cardine A, Pessa-Morikawa T, Stahls A, Fisher S, Mustelin T (1994) Induction of hyperphosphorylation and activation of the p56lck protein tyrosine kinase by phenylarsine oxide, a phosphotyrosine phosphatase inhibitor. Mol Immunol 31:1295–1302
32. Wing DR, Harvey DJ, Hughes J, Dunbar PG, McPherson KA, Paton WD (1982) Effects of chronic ethanol administration on the composition of membrane lipids in the mouse. Biochem Pharmacol 31:3431–3439
33. Mrak RE (1992) Opposite effects of dimethyl sulfoxide and ethanol on synaptic membrane fluidity. Alcohol 9:513–517
34. Laura Toppozini CLA, Barrett MA, Zheng S, Luo L, Nanda H, Sakai VG, Rheinstädter MC (2012) Partitioning of ethanol into lipid membranes and its effect on fluidity and permeability as seen by X-ray and neutron scattering. Soft Matter 8
35. Sefton BM, Trowbridge IS, Cooper JA, Scolnick EM (1982) The transforming proteins of Rous sarcoma virus, Harvey sarcoma virus and Abelson virus contain tightly bound lipid. Cell 31:465–474
36. Liang X, Nazarian A, Erdjument-Bromage H, Bornmann W, Tempst P, Resh MD (2001) Heterogeneous fatty acylation of Src family kinases with polyunsaturated fatty acids regulates raft localization and signal transduction. J Biol Chem 276:30987–30994
37. Chai X, Forster E, Zhao S, Bock HH, Frotscher M (2009) Reelin stabilizes the actin cytoskeleton of neuronal processes by inducing n-cofilin phosphorylation at serine3. J Neurosci 29:288–299
38. Flynn KC, Hellal F, Neukirchen D, Jacob S, Tahirovic S, Dupraz S, Stern S, Garvalov BK et al (2012) ADF/cofilin-mediated actin retrograde flow directs neurite formation in the developing brain. Neuron 76:1091–1107
39. Liu SL, May JR, Helgeson LA, Nolen BJ (2013) Insertions within the actin core of actin-related protein 3 (Arp3) modulate branching nucleation by Arp2/3 complex. J Biol Chem 288:487–497
40. Mullins RD, Heuser JA, Pollard TD (1998) The interaction of Arp2/3 complex with actin: nucleation, high affinity pointed end capping, and formation of branching networks of filaments. Proc Natl Acad Sci U S A 95:6181–6186
41. Piper M, Lee AC, van Horck FP, McNeilly H, Lu TB, Harris WA, Holt CE (2015) Differential requirement of F-actin and microtubule

cytoskeleton in cue-induced local protein synthesis in axonal growth cones. Neural Dev 10:3
42. Tian D, Diao M, Jiang Y, Sun L, Zhang Y, Chen Z, Huang S, Ou G (2015) Anillin regulates neuronal migration and neurite growth by linking RhoG to the actin cytoskeleton. Curr Biol 25:1135–1145
43. Ohashi K (2015) Roles of cofilin in development and its mechanisms of regulation. Develop Growth Differ 57:275–290
44. Rosario M, Schuster S, Juttner R, Parthasarathy S, Tarabykin V, Birchmeier W (2012) Neocortical dendritic complexity is controlled during development by NOMA-GAP-dependent inhibition of Cdc42 and activation of cofilin. Genes Dev 26:1743–1757
45. Moriyama K, Iida K, Yahara I (1996) Phosphorylation of Ser-3 of cofilin regulates its essential function on actin. Genes Cells 1:73–86
46. Nichols AJ, O'Dell RS, Powrozek TA, Olson EC Ex utero electroporation and whole hemisphere explants: a simple experimental method for studies of early cortical development. J Vis Exp. https://doi.org/10.3791/50271(2013)
47. Nadarajah B, Parnavelas JG (2002) Modes of neuronal migration in the developing cerebral cortex. Nat Rev Neurosci 3:423–432
48. Chai X, Fan L, Shao H, Lu X, Zhang W, Li J, Wang J, Chen S et al (2015) Reelin induces branching of neurons and radial glial cells during corticogenesis. Cereb Cortex 25:3640–3653
49. Cooper JA (2014) Molecules and mechanisms that regulate multipolar migration in the intermediate zone. Front Cell Neurosci 8:386
50. Rashid M, Belmont J, Carpenter D, Turner CE, Olson EC (2017) Neural-specific deletion of the focal adhesion adaptor protein paxillin slows migration speed and delays cortical layer formation. Development 144:4002–4014
51. Xu J, Kurup P, Foscue E, Lombroso PJ (2015) Striatal-enriched protein tyrosine phosphatase regulates the PTPalpha/Fyn signaling pathway. J Neurochem 134:629–641
52. Yokoyama N, Miller WT (2003) Biochemical properties of the Cdc42-associated tyrosine kinase ACK1. Substrate specificity, authphosphorylation, and interaction with Hck. J Biol Chem 278: 47713–47723
53. Ikeda K, Wang LH, Torres R, Zhao H, Olaso E, Eng FJ, Labrador P, Klein R et al (2002) Discoidin domain receptor 2 interacts with Src and Shc following its activation by type I collagen. J Biol Chem 277:19206–19212
54. Chai X, Zhao S, Fan L, Zhang W, Lu X, Shao H, Wang S, Song L et al (2016) Reelin and cofilin cooperate during the migration of cortical neurons: a quantitative morphological analysis. Development 143:1029–1040
55. Jossin Y, Ogawa M, Metin C, Tissir F, Goffinet AM (2003) Inhibition of SRC family kinases and non-classical protein kinases C induce a reeler-like malformation of cortical plate development. J Neurosci 23:9953–9959
56. Yip YP, Kronstadt-O'Brien P, Capriotti C, Cooper JA, Yip JW (2007) Migration of sympathetic preganglionic neurons in the spinal cord is regulated by Reelin-dependent Dab1 tyrosine phosphorylation and CrkL. J Comp Neurol 502:635–643
57. Howell BW, Gertler FB, Cooper JA (1997) Mouse disabled (mDab1): a Src binding protein implicated in neuronal development. EMBO J 16:121–132
58. Feng L, Allen NS, Simo S, Cooper JA (2007) Cullin 5 regulates Dab1 protein levels and neuron positioning during cortical development. Genes Dev 21:2717–2730
59. de Vivo L, Landi S, Panniello M, Baroncelli L, Chierzi S, Mariotti L, Spolidoro M, Pizzorusso T et al (2013) Extracellular matrix inhibits structural and functional plasticity of dendritic spines in the adult visual cortex. Nat Commun 4:1484
60. Novak U, Kaye AH (2000) Extracellular matrix and the brain: components and function. J Clin Neurosci 7:280–290
61. Popp RL, Dertien JS (2008) Actin depolymerization contributes to ethanol inhibition of NMDA receptors in primary cultured cerebellar granule cells. Alcohol 42:525–539
62. Romero AM, Esteban-Pretel G, Marin MP, Ponsoda X, Ballestin R, Canales JJ, Renau-Piqueras J (2010) Chronic ethanol exposure alters the levels, assembly, and cellular organization of the actin cytoskeleton and microtubules in hippocampal neurons in primary culture. Toxicol Sci 118:602–612
63. Romero AM, Renau-Piqueras J, Pilar Marin M, Timoneda J, Berciano MT, Lafarga M, Esteban-Pretel G (2013) Chronic alcohol alters dendritic spine development in neurons in primary culture. Neurotox Res 24:532–548
64. dos Remedios CG, Chhabra D, Kekic M, Dedova IV, Tsubakihara M, Berry DA, Nosworthy NJ (2003) Actin binding proteins: regulation of cytoskeletal microfilaments. Physiol Rev 83:433–473
65. Wang X, Qiu R, Tsark W, Lu Q (2007) Rapid promoter analysis in developing mouse brain and genetic labeling of young neurons by doublecortin-DsRed-express. J Neurosci Res 85:3567–3573
66. Nichols AJ, Olson EC (2010) Reelin promotes neuronal orientation and dendritogenesis during preplate splitting. Cereb Cortex 20: 2213–2223
67. O'Dell R, Ustine CM, Lawless SM, Cameron DA, Williams CM, Zipfel WR, Olson EC (2011) Dendritogenesis and orientation of Layer 6 cortical neurons during early cortical development. Society for Neuroscience, Washington D.C.